ISSN 1674-1056
http://cpb.iphy.ac.cn
http://iopscience.iop.org/cpb
中国物理 B
Chinese Physics
中国物理 Chinese Physics B

Visualization of tunnel magnetoresistance effect in single manganite nanowires

Yang Yu(郁扬)[1], Wenjie Hu(胡雯婕)[1], Qiang Li(李强)[1], Qian Shi(时倩)[1], Yinyan Zhu(朱银燕)[1], Hanxuan Lin(林汉轩)[1], Tian Miao(苗田)[1], Yu Bai(白羽)[1], Yanmei Wang(王艳梅)[1], Wenting Yang(杨文婷)[1], Wenbin Wang(王文彬)[2], Hangwen Guo(郭杭闻)[2], Lifeng Yin(殷立峰)[1,2,3], Jian Shen(沈健)[1,2,3]

Citation: Chin. Phys. B . 2020, 29(1): 018501 . **doi:** 10.1088/1674-1056/ab5932
Journal homepage: http://cpb.iphy.ac.cn; http://iopscience.iop.org/cpb

What follows is a list of articles you may be interested in

Analysis of non-uniform hetero-gate-dielectric dual-material control gate TFET for suppressing ambipolar nature and improving radio-frequency performance

Hui-Fang Xu(许会芳), Jian Cui(崔健), Wen Sun(孙雯), Xin-Feng Han(韩新风)
Chin. Phys. B . 2019, 28(10): 108501 . **doi:** 10.1088/1674-1056/ab3a8b

Double-gate-all-around tunnel field-effect transistor

Wen-Hao Zhang(张文豪), Zun-Chao Li(李尊朝), Yun-He Guan(关云鹤), Ye-Fei Zhang(张也非)
Chin. Phys. B . 2017, 26(7): 078502 . **doi:** 10.1088/1674-1056/26/7/078502

Characteristics of cylindrical surrounding-gate $GaAs_xSb_{1-x}/In_yGa_{1-y}As$ heterojunction tunneling field-effect transistors

Yun-He Guan(关云鹤), Zun-Chao Li(李尊朝), Dong-Xu Luo(骆东旭), Qing-Zhi Meng(孟庆之), Ye-Fei Zhang(张也非)
Chin. Phys. B . 2016, 25(10): 108502 . **doi:** 10.1088/1674-1056/25/10/108502

Breakdown voltage model and structure realization of a thin silicon layer with linear variable doping on a silicon on insulator high voltage device with multiple step field plates

Qiao Ming, Zhuang Xiang, Wu Li-Juan, Zhang Wen-Tong, Wen Heng-Juan, Zhang Bo, Li Zhao-Ji
Chin. Phys. B . 2012, 21(10): 108502 . **doi:** 10.1088/1674-1056/21/10/108502

RAPID COMMUNICATION

Visualization of tunnel magnetoresistance effect in single manganite nanowires*

Yang Yu(郁扬)[1,†], Wenjie Hu(胡雯婕)[1,†], Qiang Li(李强)[1,†], Qian Shi(时倩)[1], Yinyan Zhu(朱银燕)[1], Hanxuan Lin(林汉轩)[1], Tian Miao(苗田)[1], Yu Bai(白羽)[1], Yanmei Wang(王艳梅)[1], Wenting Yang(杨文婷)[1], Wenbin Wang(王文彬)[2], Hangwen Guo(郭杭闻)[2,‡], Lifeng Yin(殷立峰)[1,2,3,§], and Jian Shen(沈健)[1,2,3,¶]

[1] *State Key Laboratory of Surface Physics and Department of Physics, Fudan University, Shanghai* 200433, *China*
[2] *Institute for Nanoelectronic Devices and Quantum Computing, Fudan University, Shanghai* 200433, *China*
[3] *Collaborative Innovation Center of Advanced Microstructures, Nanjing* 210093, *China*

(Received 16 November 2019; accepted manuscript online 20 November 2019)

We reported a study of tunnel magnetoresistance (TMR) effect in single manganite nanowire via the combination of magnetotransport and magnetic force microscopy imaging. TMR value up to 290% has been observed in single $(La_{1-y}Pr_y)_{1-x}Ca_xMnO_3$ nanowires with varying width. We find that the TMR effect can be explained in the scenario of opening and blockade of conducting channels from inherent magnetic domain evolutions. Our findings provide a new route to fabricate TMR junctions and point towards future improvements in complex oxide-based TMR spintronics.

Keywords: manganite nanowires, tunnel magnetoresistance, magnetic force microscope

PACS: 85.30.Mn, 07.79.Pk, 71.27.+a **DOI:** 10.1088/1674-1056/ab5932

1. Introduction

Over the past decades, tunnel magnetoresistance (TMR) effect has attracted lots of research interests due to its conceptual importance in spintronics and potential of technological applications.[1–4] One of the most well-known geometries to fabricate TMR architectures is the magnetic tunnel junction (MTJ).[5–7] The basic structure of a MTJ usually consists of a thin insulating layer sandwiched between two ferromagnetic electrode layers. Depending on the relative spin orientation of the two ferromagnetic electrodes being parallel or antiparallel, the low/high resistance state (R_P/R_{AP}) can be achieved. Such structure has proven to be successful, but carries complications in materials synthesis because controlled growth of multiple materials is required. This unavoidably mandates extra care in the growth process, since different materials can have different optimal thermodynamic growth parameters and their interfaces can have dramatic impacts on the TMR properties.[8,9]

An alternative approach to achieve TMR effect is to utilize the intrinsic coexistence of different electronic phases in complex oxide systems. Perovskite manganites such as $(La_{1-y}Pr_y)_{1-x}Ca_xMnO_3$ (LPCMO) provide a good platform. The interaction of electron, spin, orbital, and lattice produces the rich phases in the system, such as the emergence of antiferromagnetic charge ordered insulating (COI) phase and ferromagnetic metallic (FMM) phase. These phases can coexist at wide ranges of temperatures and magnetic fields, effectively having the opportunity to form intrinsic FMM/COI/FMM junction with TMR effect. Such intrinsically formed junctions have the merit of eliminating chemical interfaces, thus the fabrication of multiple layers is not required. Although TMR effects have been observed in LPCMO nanowires and antidots systems and several mechanisms and models have been proposed,[10–14] a clear TMR-based FMM/COI/FMM feature has not been observed, clouding the underlying mechanism on the TMR effect.

In this work, we study the TMR effect in LPCMO nanowires with a particular emphasis on the underlying mechanism. The magnetic force microscope (MFM) measurements directly visualized the magnetic domain evolutions under magnetic fields. Combining with the magnetotransport measurements, we conclude that the TMR effects can be understood in the scenario of opening and blockage of filamentary conducting channels in FMM/COI/FMM domain configurations. Such mechanism is completely different from that in the traditional TMR junctions and can be only realized under spatially confined nanowires.

2. Method

A 30 nm $(La_{2/3}Pr_{1/3})_{5/8}Ca_{3/8}MnO_3$ (LPCMO) thin film sample is grown by pulse laser deposition (PLD) on a $LaAlO_3$

*Project supported by the National Key Research and Development Program of China (Grant No. 2016YFA0300702), Shanghai Municipal Natural Science Foundation, China (Grant Nos. 19ZR1402800, 18JC1411400, 18ZR1403200, and 17ZR1442600), the Program of Shanghai Academic Research Leader, China (Grant Nos. 18XD1400600 and 17XD1400400), and the China Postdoctoral Science Foundation (Grant Nos. 2016M601488 and 2017T100265).

†These authors contributed equally to this work.
‡Corresponding author. E-mail: hangwenguo@fudan.edu.cn
§Corresponding author. E-mail: lifengyin@fudan.edu.cn
¶Corresponding author. E-mail: shenj5494@fudan.edu.cn

© 2020 Chinese Physical Society and IOP Publishing Ltd

(001) substrate. The substrate is heated to 800 ℃ in the atmosphere of 8×10^{-1} Pa oxygen containing 8% ozone. Reflection high-energy electron diffraction (RHEED) is used to ensure the high quality of layer-by-layer epitaxial growth via its oscillations of intensity during sample growth. After growth, the sample is post annealed at 850 ℃ for 3 h in 1 atmosphere oxygen to minimize the influence of oxygen vacancies. Nanofabrication techniques are employed to fabricate LPCMO nanowires. The LPCMO nanowires are fabricated by electron beam lithography. 200 nm AR-N 7520, a negative E-beam resist, is covered on the thin film by spin-coating. Electron beam lithography (Zeiss SIGMA SEM and Raith Elphy Plus pattern processor) is employed to pattern the wires on the negative resists. Developing liquid ($RZX3038 : H_2O = 4 : 1$) is used to remove the part without electron beam writing after patterning. Argon ion beam etching is applied to corrode the part uncovered by resist and retain the nanowires pattern. Reactive-ion etching with oxygen plasma is applied to remove the residual resist. At last, the LPCMO naonwire is patterned with gold electrodes by optical lithography.

The length of the wires is 20 μm. These straight wires have smooth edges, indicating high quality of the sample after nanofabrication. The electronic transport is measured by a physical property measurement system (PPMS) with 2-probe connection. The current density through the nanowires is controlled around 3×10^3 A/cm^2, using the source Agilent 2900 series, in order to reduce the effect of current-induced heating.

3. Result and discussion

Figure 1 shows the electrical transport behavior of a 400 nm nanowire during the cooling process at 0 T. The morphology of the nanowire is shown in the inset of Fig. 1. With decreasing temperature, the LPCMO nanowire undergoes the paramagnetic insulator (PI) to charge order insulator (COI) transition, then the FMM state domains begin to form and grow when the temperature is lower, resulting in the decrease of resistance. According to previous reports,[15–17] the FMM and COI domains coexist in a wide range of temperature. Since the typical length scales of these domains are usually 300–400 nm,[16] the spatial confinement allows only few percolation path for the conducting electrons to pass through. This effect is also reflected by the sudden resistance jumps during the COI to FMM transition observed in Fig. 1.

Figure 2 shows the typical TMR behavior of the 400 nm LPCMO nanowire at 108 K under a magnetic field along surface normal. The external magnetic field is first set at 3000 Oe and swept towards −3000 Oe. At 3000 Oe, the nanowire is in a low resistance state. Upon decreasing the magnetic field, the resistance remains at a low value until the field reaches about 1500 Oe. Below 1500 Oe, the resistance starts to increase continuously with obvious enhancement of fluctuation. Such fluctuation can be understood in the scenario of enhanced inherent competition between COI and FMM states.[18]

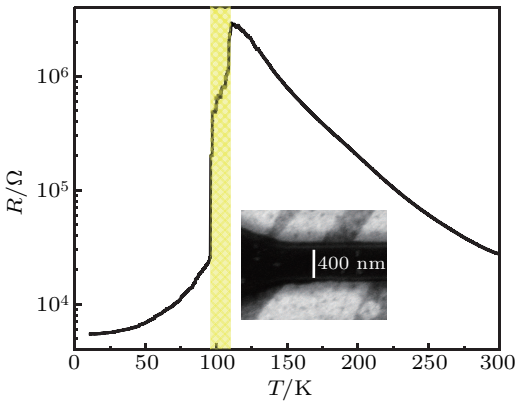


Fig. 1. Resistivity vs. temperature measurements of 400 nm LPCMO nanowires under cooling at 0 T. The inset shows the SEM images of the 400 nm nanowires.

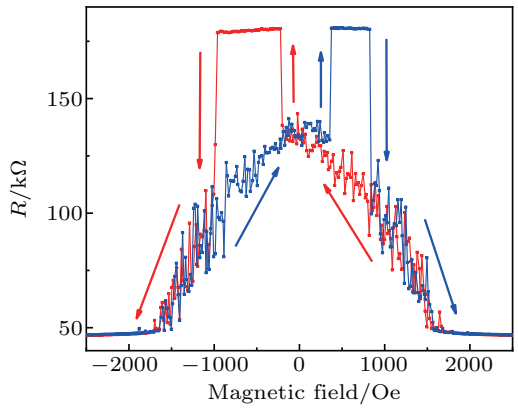


Fig. 2. Resistivity vs. magnetic field measurements of 400 nm LPCMO nanowires after cooling to 108 K. Red and blue curves and arrows correspond to the changes of magnetic field from +3000 Oe to −3000 Oe and −3000 Oe to +3000 Oe, respectively.

When the magnetic field reaches −200 Oe, a sudden jump of resistance to a higher value occurs. The resistance remains stable at this high value until the magnetic field reaches −900 Oe, at which the resistance of the nanowire drops abruptly to a lower value and then decreases continuously. When sweeping the magnetic field from −3000 Oe to 3000 Oe, a similar behavior is observed with the corresponding upward and downward jumps of the resistance occurring at 400 Oe and 800 Oe, respectively. The MR ratio is calculated as $\mathrm{MR} = (R - R_{0.3\mathrm{T}})/R_{0.3\mathrm{T}}$, and it reaches 290%. Such TMR effects are observed in the temperature range between 96 K and 111 K as highlighted in Fig. 1. This temperature range corresponds to the regime where the COI and FMM competition is the strongest.

The domain evolution during the TMR process is directly visualized in a 500 nm nanowire using MFM with different applied magnetic fields along surface normal, as shown in Fig. 3. The morphology of this nanowire is shown by atomic force microscope (AFM) in Fig. 3(a). The MFM images are acquired in the range from −1000 Oe to 1000 Oe where TMR is typically observed. The temperature is fixed at 110 K and the

magnetic field is first set at 1000 Oe. At 1000 Oe, most areas are in FMM state (red) as shown in Fig. 3(b). When decreasing the magnetic field to 0 Oe, some blue areas begin to nucleate and grow in size. When the magnetic field varies from 0 Oe to −300 Oe, the blue domains continue to grow and cover the full width of the nanowire. With further increasing negative field, the domains in the nanowire turn uniform again at −1000 Oe. Note that at −1000 Oe, the domains are in red color due to the fact that the MFM tip with coercive field around 700 Oe has flipped its magnetization direction and became parallel with the domains' spin direction (as illustrated in Fig. 4). Similar domain evolution process is observed when the magnetic field is swept from −1000 Oe back to 1000 Oe.

We now turn to discuss the correlation between the MFM and transport measurements during the TMR process. We first identify the nature of the observed blue domains which nucleate with decreasing magnetic field. Based on the imaging principle of MFM, these blue domains may correspond to either COI domains or the FMM domains with the magnetization direction antiparallel to the MFM tip. For manganites, it is well established that the magnetic field can melt the COI state into FMM state. The fact that the blue domains continue to grow with increasing field from 0 to −300 Oe (Figs. 3(e) and 3(f)) in our nanowire effectively rules out the possibility of them being COI domains. Therefore, we conclude that the blue domains are in the FMM state with spin antiparallel to the red domains.

Figure 4 represents a plausible mechanism in explaining the observed TMR effect. The enlarged views of the same area under different fields from Fig. 3 are shown along with the tip/domain configurations. At 1000 Oe (Fig. 4(a)), the nanowire is in a uniform ferromagnetic state with spin direction of domains parallel to that the tip (defined as spin-up domains). In this state, the electrons can transport through this area freely, resulting in the low resistance state. When the magnetic field decreases, blue domains with spin direction antiparallel to the tip (spin-down domains) start to nucleate and grow (Fig. 4(b)). At this stage, the electrons experience enhanced scattering across the whole nanowire from the interfaces between the spin-up and spin-down domains, but the spin-up domains are still percolated along the nanowire. Therefore, the overall resistance increases in a continuous manner. When the magnetic field increases to about −300 Oe (Fig. 4(c)), the spin-down domain becomes large enough to cover the full width of the nanowire, effectively blocking the existing percolation channels. This forms the MTJ structure for the electrons to tunnel, so the resistance of the nanowire jumps to a large value. We note that due to the MFM resolution limit, we could not identify the exact nature of the thin insulating barrier (white region) between the spin-up and spin-down domains. However, at this temperature regime, the COI state should still be present between the FMM domains so we speculate that the thin white area is COI domains. When further increasing the negative magnetic field, the spin-down domains are large enough to percolate through the nanowire, opening up a percolation channel so that the system recovers to a low-resistance state, as shown in the case of Fig. 4(d). This process is qualitatively reproduced when sweeping the field from −1000 Oe to 1000 Oe (Figs. 4(e)–4(h)).

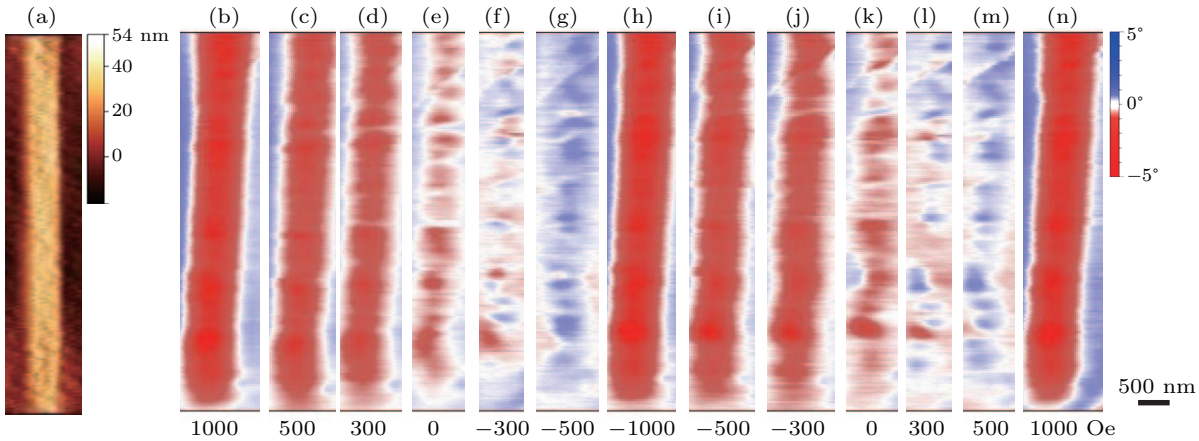


Fig. 3. MFM measurements of 500 nm LPCMO nanowire during the TMR process at 110 K. (a) AFM image of the 500 nm nanowires. (b)–(n) MFM images of 500 nm LPCMO at different magnetic fields. The magnetic field was varied following the order from (b) to (n). Red area corresponds to the FMM domains with spin parallel to the tip, blue area corresponds to the FMM domains with spin antiparallel to the tip, as illustrated in details in Fig. 4.

The above results illustrate that the TMR effect observed in a single manganite wire is of distinctively different nature from that of the conventional TMR junctions which consist of three different layers of materials. From application point of view, two issues need to be resolved for the single nanowire TMR in manganites. First, since the domain distributions are random and different at each thermal cycle,[19,20] the TMR effects are not always repeatable under different temperature cycles, as observed in several publications[10,11,14] and our work here. Therefore, it is important to develop strategies to ob-

tain TMR structures with well-defined domain positions and sizes in order to gain better control of the TMR effect. Local electric-field gating[21] or magnetic patterning[22] can be possible solutions. Second, from application point of view, it is essential to elevate the operation temperature by developing new materials or new heterostructures.[23]

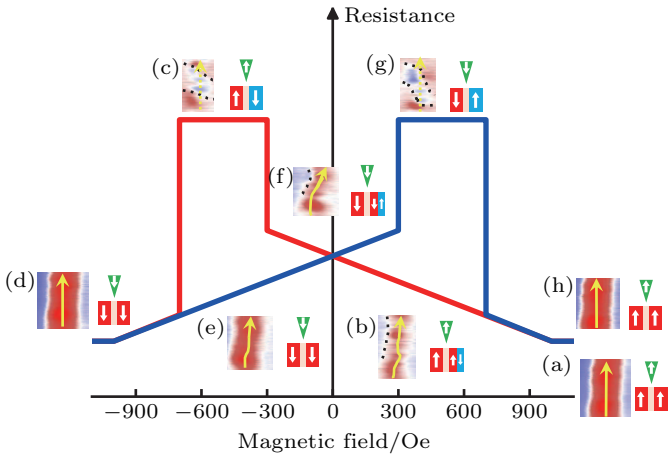


Fig. 4. The schematic interpretation of TMR effect. (a)–(h) MFM images of the 500 nm LPCMO nanowire in the same area during the TMR process at 110 K on the sequence of (a) 1000 Oe, (b) 0 Oe, (c) −300 Oe, (d) −1000 Oe, (e) −300 Oe, (f) 0 Oe, (g) 300 Oe, (h) 1000 Oe from Fig. 3. The magnetic field was swept following the above order. The black dash lines in the MFM images represent the blockade between the nearby antiparallel magnetic domains. The solid yellow arrows represent the conducting path for electrons, and the dashed yellow arrows represent the tunneling of the electrons. The cartoon besides every MFM image shows the relative directions of MFM tip and magnetic domains. The red and blue curves represent the schematic of resistance states with magnetic field changing from 1000 Oe to −1000 Oe and −1000 Oe to 1000 Oe, respectively.

4. Conclusion

In summary, via the combination of nanofabrication, magnetotransport, and MFM imaging, we achieve large TMR effect in single manganite nanowires and propose a plausible mechanism. Our research provides a new route to design TMR devices based on electronic phase separated systems without chemical interfaces.

References

[1] Fert A 2008 *Rev. Mod. Phys.* **80** 1517
[2] Wolf S A, Awschalom D D, Buhrman R A, Daughton J M, Von Molnár S, Roukes M L, Chtchelkanova A Y and Treger D M 2001 *Science* **294** 1488
[3] Žutić I, Fabian J and Das Sarma S 2004 *Rev. Mod. Phys.* **76** 323
[4] Yuasa S, Nagahama T, Fukushima A, Suzuki Y and Ando K 2004 *Nat. Mater.* **3** 868
[5] Tsymbal E Y, Mryasov O N and Leclair P R 2003 *J. Phys.: Condens. Matter* **15** R109
[6] Moodera J S and Mathon G 1999 *J. Magn. Magn. Mater.* **200** 248
[7] Ikeda S, Hayakawa J, Lee Y M, Matsukura F, Ohno Y, Hanyu T and Ohno H 2007 *IEEE Trans. Electron. Devices* **54** 991
[8] De Teresa J M, Barthélémy A, Fert A, Contour J P, Montaigne F and Seneor P 1999 *Science* **286** 507
[9] Ishii Y, Yamada H, Sato H, Akoh H, Ogawa Y, Kawasaki M and Tokura Y 2006 *Appl. Phys. Lett.* **89** 042509
[10] Singh-Bhalla G, Biswas A and Hebard A F 2009 *Phys. Rev. B* **80** 144410
[11] Li H, Li L, Li L, Liang H, Cheng L, Zhai X and Zeng C 2014 *Appl. Phys. Lett.* **104** 082414
[12] Jeon J, Jung J and Chow K H 2017 *Appl. Phys. Lett.* **111** 242401
[13] Jeon J, Jung J and Chow K H 2017 *Nanoscale* **9** 19304
[14] Jeon J, Jung J and Chow K H 2017 *J. Phys. Soc. Jpn.* **86** 084705
[15] Zhang L, Israel C, Biswas A, Greene R L and De Lozanne A 2002 *Science* **298** 805
[16] Uehara M, Mori S, Chen C H and Cheong S W 1999 *Nature* **399** 560
[17] Kim K H, Uehara M, Hess C, Sharma P A and Cheong S W 2000 *Phys. Rev. Lett.* **84** 2961
[18] Ward T Z, Zhang X G, Yin L F, Zhang X Q, Liu M, Snijders P C, Jesse S, Plummer E W, Cheng Z H, Dagotto E and Shen J 2009 *Phys. Rev. Lett.* **102** 087201
[19] Kundhikanjana W, Sheng Z, Yang Y, Lai K, Ma E Y, Cui Y T, Kelly M A, Nakamura M, Kawasaki M, Tokura Y, Tang Q, Zhang K, Li X and Shen Z X 2015 *Phys. Rev. Lett.* **115** 265701
[20] Zhai H Y, Ma J X, Gillaspie D T, Zhang X G, Ward T Z, Plummer E W and Shen J 2006 *Phys. Rev. Lett.* **97** 167201
[21] Guo H, Noh J H, Dong S, Rack P D, Gai Z, Xu X, Dagotto E, Shen J and Ward T Z 2013 *Nano Lett.* **13** 3749
[22] Ward T Z, Gai Z, Xu X Y, Guo H W, Yin L F and Shen J 2011 *Phys. Rev. Lett.* **106** 157207
[23] Zhu Y, Du K, Niu J, Lin L, Wei W, Liu H, Lin H, Zhang K, Yang T, Kou Y, Shao J, Gao X, Xu X, Wu X, Dong S, Yin L and Shen J 2016 *Nat. Commun.* **7** 11260